High Accuracy and Fast Speed MPPT Methods for PV String Under Partially Shaded Conditions

Yunping Wang, Ying Li, *Student Member*, *IEEE*, Xinbo Ruan, *Senior Member*, *IEEE*

***Abstract*—The photovoltaic (PV) string under partially shaded conditions exhibits complex output characteristics, i.e., the current-voltage (*I-V*) curve presents multiple current stairs while the power-voltage (*P-V*) curve shows multiple power peaks. Thus, the conventional maximum power point tracking (MPPT) method is not acceptable either on tracking accuracy or on tracking speed. In this paper, two global MPPT methods, namely, the search-skip-judge global MPPT (SSJ-GMPPT) and rapid global MPPT (R-GMPPT) methods are proposed in term of reducing the searching voltage range based on comprehensive study of I-V and P-V characteristics of PV string. The SSJ-GMPPT method can track the real maximum power point (MPP) under any shading conditions and achieve high accuracy and fast tracking speed without additional circuits and sensors. The R-GMPPT method aims to enhance the tracking speed of long string with vast PV modules, and reduces more than 90% of the tracking time that is consumed by the conventional global searching method. The improved performance of two proposed methods have been validated by experimental results on a PV string. The comparison with other methods highlights the two proposed methods more powerful.**

***Index Terms*—Photovoltaic generation system, maximum power point tracking (MPPT), partially shaded conditions (PSC), global maximum power point (GMPP)**

I. Introduction

With concerns on energy crisis and environmental pollution, great attentions have been paid to solar energy due to its advantage as an inexhaustible and environment-friendly energy supply [1]. Photovoltaic (PV) module is one of the majority patterns to harvest solar energy. In order to generate sufficient electric power, multiple PV modules are often connected in series or parallel to form a PV string or array. PV string is the prior configuration of PV modules in term of the lowest mismatch power losses due to nonhomogeneous irradiance [2], [3].

It is preferable to operate PV string at the maximum power point (MPP) to sufficiently extract PV energy [4]. The conventional well-known MPP tracking (MPPT) methods include perturbation and observation (P&O) and incremental conductance (IncCond) [5]. Since the power-voltage (*P-V*) curve of PV string has one MPP under uniform irradiance, these conventional methods can track the MPP accurately. With non-uniform irradiance, resulted by trees, buildings and clouds shadow nearby, the *P-V* curve of a PV string exhibits multiple peak-power points (PPPs), in which one is the global MPP (GMPP) and the other are the local MPPs (LMPPs), and the conventional methods hardly differentiate between GMPP and LMPP, therefore reducing the overall efficiency of PV string. A survey reported that the operation of 41% installed PV systems had been affected by shadow, with energy losses of 10% [6]. The searching process within full voltage range can guarantee the tracking accuracy of GMPP, however, the tracking process is time-consuming. So, it is necessary to develop the MPPT method with ability to fast track the GMPP under partially shaded conditions (PSC).

To date, abundant literatures have been published to address the MPPT issue under PSC which are based on hardware and software solutions, respectively. The hardware methods include circuit compensation and reconfiguration. The circuit compensation method uses additional circuit to eliminate the multiple peaks, so the P-V curve exhibits only one peak even under PSC, thus the conventional MPPT methods can be used [7-10]. However, the additional circuit increases the system complexity and can not be adjusted flexibly corresponding to different PV configurations. The method of reconfiguration has been developed in [11-13], which is using a matrix of power switches to recombine the individual PV modules in a PV array. The target of this reconfiguration is to form the PV modules comprised by the PV array operating under similar solar irradiance conditions. With this method, the complexity of the system configuration and cost are significantly increased [6].

The software MPPT methods under PSC can be categorized into three groups. In the first group, several intelligent algorithms, such as particle swarm optimization (PSO) [14]–[16], flashing fireflies [17], artificial bee colony [18], fuzzy-logic control [19], chaotic search [20], are proposed to being used in PV system. The advantages of intelligent algorithms are their adaptive ability of accurately tracking GMPP regardless of shading patterns, P-V characteristic and the configuration of PV array. However, the intelligent algorithms are complex to implement and the initial point must be carefully selected by professional. The second group includes three fast MPPT methods, i.e., load-line method [21], [22], DIRECT method [23], and a method based on Fibonacci technique [24]. The fast MPPT methods can track the MPP with a fast speed but the tracking result may be one of the LMPPs rather than the GMPP. The third group is the specifically improved MPPT methods based on conventional search algorithms. These methods utilize the unique characteristics of the PV systems under PSC to track the GMPP and can be realized simply by modifying the conventional MPPT algorithms. Thus, these methods may be more preferable in that they do not increase component count of the system. In [25], a deterministic change to PSO method improves the tracking speed. The deterministic change is based on the critical study of PV characteristics under PSC. A modified incremental conductance algorithm is proposed

Manuscript received December 23, 2014; revised April 5, 2015 and May 30, 2015; accepted June 20, 2015.

This work was supported by the Fundamental Research Funds for the Central Universities NS2015035.

The authors are with the Aero-Power Sci-tech Center, the College of Automation Engineering, Nanjing University of Aeronautics and Astronautics, Nanjing 210016, China (e-mail: wyp@nuaa.edu.cn; liying1992@nuaa.edu.cn; ruanxb@nuaa.edu.cn;).

This article has been accepted for publication in a future issue of this journal, but has not been fully edited. Content may change prior to final publication. Citation information: DOI 10.1109/TIE.2015.2465897, IEEE Transactions on Industrial Electronics

based on a comprehensive study which shows that peaks in P-V curve occur approximately at the multiples of 80% of open-circuit (OC) voltage [26-31]. However, the modified incremental conductance is time-consumed for application of PV long string because the method searches all the vicinity of PPPs. Recently a GMPP tracking method, which restricts the voltage window (VW) search range and tracks the GMPP in all shading conditions, is proposed [2]. By means of restricting the voltage window search range the tracking speed is improved. It is a pity for VW method that the characteristic of PV string is not considered and therefore its tracking speed is not fast enough yet.

As previously mentioned, the MPPT methods under PSC have more or less disadvantages in terms of tracking accuracy, tracking speed and implementing complexity [32]. The critical issue for PV string MPPT scheme is reducing the searching voltage range by skipping the unnecessary voltage intervals according to the unique P-V characteristic. The improvement of tracking speed mainly depends on the degree of reducing voltage searching range.

This paper proposes two global MPPT methods under PSC based on the P-V and I-V curve of PV string. The first method can track the real GMPP in any shading pattern with approving tracking speed, and the implementation is simple because it does not require the knowledge of output electrical characteristic of PV string and any additional voltage and current sensors. The second method is designed with very fast tracking speed to apply on long PV string. In these two methods, the searching voltage range is significantly reduced and tracking accuracy is approving as well. The two methods are realized with the specifically improved changes based on the conventional IncCond method. After the vicinity of the GMPP is obtained the conventional IncCond method is used to find real GMPP without oscillation at steady state. This paper is organized as follows. In Section II, the output electrical characteristics (I-V curve and *P-V* curve) of the PV string is investigated, and two relations are achieved. One relation is that the PPP-current is approximately proportional to the short-circuit current (SC-current), I_{sc}, and the other is that the PPP voltage is approximately proportional to the open-circuit voltage (OC-voltage), V_{oc}. In Sections III, based on the first relation, a search-skip-judge global MPPT (SSJ-GMPPT) method is proposed. The algorithm operating process is analyzed with regard to different shading patterns. Based on the second relation, a rapid global MPPT (R-GMPPT) is proposed in Sections IV. In Section V the experimental results are presented to demonstrate the effectiveness of the two proposed methods. And the performance of the proposed two methods is compared with the modified incremental conductance algorithm in [27]. Finally, Section VI concludes this paper.

II. Output Characteristic of PV String

A. Output Characteristics of PV String under Uniform Irradiance

Fig. 1(a) shows the equivalent circuit of a PV module, and Fig. 1(b) shows the output characteristics including the *I-V* curve and *P-V* curve [33]. As is shown, the *P-V* curve exhibits only one PPP, the MPP. On the left side of the MPP the PV module outputs approximately constant current, while it outputs approximately constant voltage on the right side of the MPP. The current and voltage of MPP (I_m and V_m) can be approximately expressed as [34]:

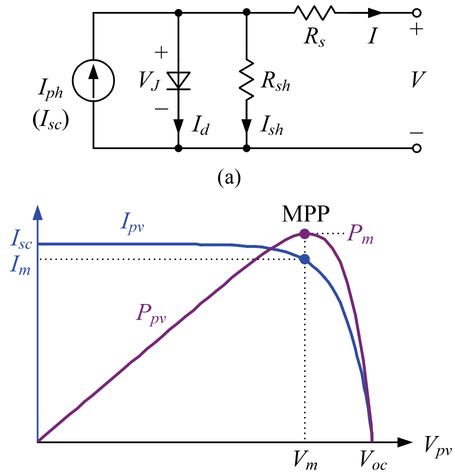

Fig. 1. PV module: (a). Equivalent circuit. (b). P-V and I-V curves.

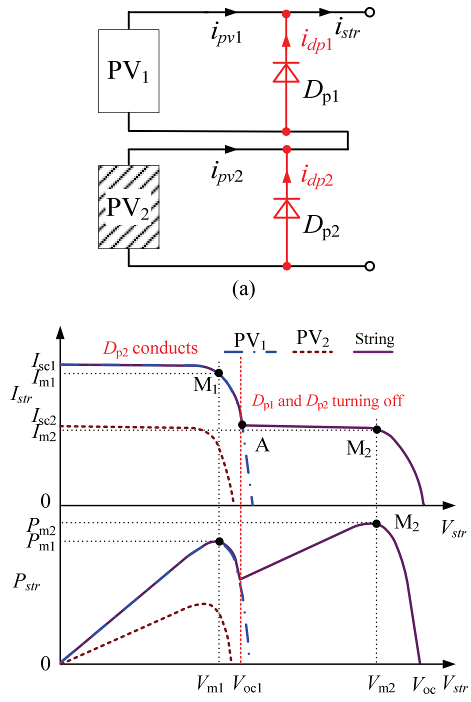

Fig. 2. Two PV modules in series under PSC. (a) Circuit configuration. (b) Output characteristic curves.

$$I_{\mathrm{m}} \approx 0.9 I_{\mathrm{sc}} \tag{1}$$

$$V_{\mathrm{m}} \approx 0.76 V_{\mathrm{oc}} \tag{2}$$

Multiple PV modules can be connected in series to constitute one PV string. Under uniform irradiance (UI), these PV modules have the same output characteristics, thus, the output characteristic of PV string is simply obtained by those of PV modules. Likely, the current and voltage of MPP ($I_{\mathrm{m\_str}}$ and $V_{\mathrm{m\_str}}$) can be expressed as:

$$I_{\mathrm{m\_str}} \approx 0.9 I_{\mathrm{sc\_str}} \tag{3}$$

$$V_{\mathrm{m\_str}} \approx 0.76 V_{\mathrm{oc\_str}} \tag{4}$$

where, $I_{\mathrm{sc\_str}}$ is the SC-current and $V_{\mathrm{oc\_str}}$ is the OC-voltage of PV string.

B) Output Curves of PV String with Two PV Modules under

PSC

The PV string with two modules is shown in Fig. 2(a). It is assumed that PV_1 receives more irradiance than PV_2, so the SC-current and OC-voltage of PV_1 are larger than those of PV_2 [35]. Fig. 2(b) shows the output curves of the PV string. When the string current, i_{str}, is smaller than the SC-current of PV_2, I_{sc2}, both PV_1 and PV_2 generate energy and the string voltage is equal to the sum of voltages of PV_1 and PV_2. When i_{str} exceeds I_{sc2}, diode D_{p2} conducts, and thus, PV_2 is bypassed and does not generate energy. Then, the output of string is equal to that of PV_1.

As seen in Fig. 2(b), the *I-V* curve of PV string presents two stairs and the *P-V* curve of PV string has two PPPs, i.e., M_1 and M_2. Point A is the dividing point. On the left of point A, only PV_1 works, and the PPP-current I_{m1} is approximately equal to $0.9{\cdot}I_{sc1}$, and the PPP-voltage V_{m1} is approximately equal to $0.76{\cdot}V_{oc1}$. On the right of point A, PV_1 and PV_2 work together. Because PV_1 generates approximately constant voltage and the turning point of *I-V* curve is mainly affected by PV_2, the PPP-current I_{m2} is approximately equal to $0.9{\cdot}I_{sc2}$, and the PPP-voltage V_{m2} is approximately equal to the sum of V_{oc1} and $0.76{\cdot}V_{oc2}$. The OC-voltage is proportional to the natural logarithm of illumination intensity [35], so V_{oc1} is approximately equal to V_{oc2}, which is equal to half of the OC-voltage of PV string, V_{oc}. That is, $V_{m1} = 0.76{\cdot}V_{oc}/2$, $V_{m2} = (1{+}0.76){\cdot}V_{oc}/2$.

Similarly, for the *n* PV modules connected in series under PSC, the *I-V* curve has *n* stairs, and the P-V curve shows *n* divided intervals, and every interval has one PPP. Thus, the *P-V* curve has *n* PPPs. The PPP-current and PPP-voltage of *No.j* ($j = 1, 2, \ldots, n$), I_{mj} and V_{mj}, are expressed as:

$$I_{mj} \approx 0.9 I_{scj} \tag{5}$$

$$V_{mj} \approx (j-1+0.76)V_{oc}/n = (j-0.24)V_{oc}/n \tag{6}$$

where I_{scj} and V_{ocj} are the SC-current and OC-voltage of *No.j* PV module, respectively. It should be noted that the relation is developed only the irradiance difference is considered in (5) and (6). In fact the OC-voltage is affected also by the PV module temperature. The precise output characteristic of PV string under PSC and different temperatures can be found in [36].

III. Search-Skip-Judge Global MPPT Method

For the conventional global MPPT method, it is necessary to scan the full voltage range from zero to the OC-voltage to obtain the GMPP. However, the searching voltage range should be reduced by utilized the characteristic of PV string under PSC. In this section reducing the searching voltage range is realized by skipping the vicinity of the LMPPs based on (5). This method is the search-skip-judge global MPPT (SSJ-GMPPT) method which fast tracks the real GMPP without additional circuit and voltage or current sensor (only one pair of voltage and current sensors required as the conventional methods).

In order to help understanding the operating principle of the SSJ-GMPPT method, a PV string with three modules is taken as an example to illustrate the whole operating process. The irradiance levels of three modules are intentionally given to be different, and the P-V curve of string has three PPPs, M_1, M_2 and M_3, as shown in Fig. 3. Fig. 3(a), (b) and (c) show three shading patterns, in which M_1, M_2 and M_3 is the GMPP, respectively.

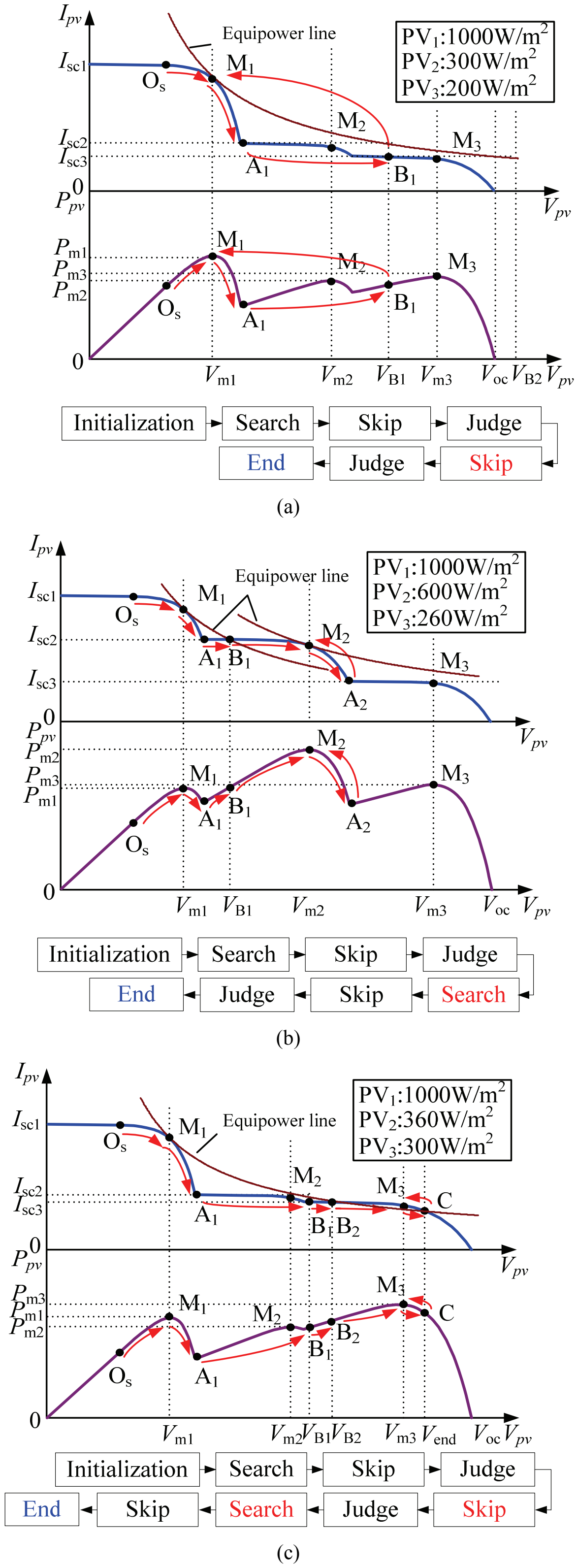

Fig. 3. Tracking process of SSJ-GMPPT method for string with three PV modules under PSC. (a) pattern 1, (b) pattern 2, (c) pattern 3.

Fig. 4 gives the block diagram of the SSJ-GMPPT, where $V_{oc\text{-}mod}$ is the OC-voltage of a single module and it is available in the typical parameters provided by the manufacturer. P_m is the global maximum power recorded in tracking process and V_m is the voltage corresponding to P_m, ΔV is the incremental voltage in every perturbation, *n* is the number of module in series, and I_{scj} represents the SC-current of the *j*th module, which is exactly the current of section-dividing point (SDP)

This article has been accepted for publication in a future issue of this journal, but has not been fully edited. Content may change prior to final publication. Citation information: DOI 10.1109/TIE.2015.2465897, IEEE Transactions on Industrial Electronics

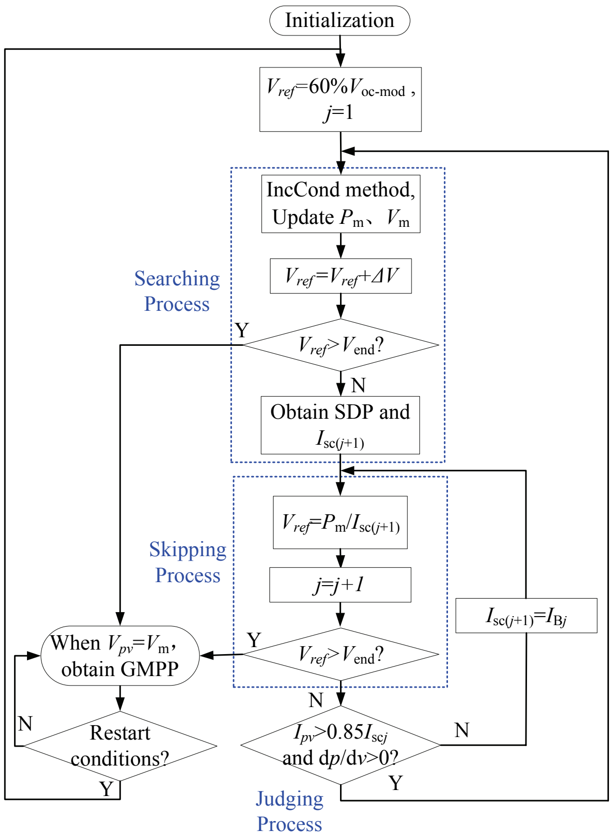

Fig. 4. Complete algorithm flowchart of SSJ-GMPPT.

between current stairs in *I-V* curve [12]. Generally, the number of SDPs and PPPs are both equal to *n*.

The initial operating voltage is set to 60% of $V_{oc\text{-}mod}$ to guarantee that the first PPP (M_1 in Fig. 3) can be found. 90% OC-voltage of the string is set as the ending voltage (V_{end}) since no MPP will appear when the operating voltage is higher than 90% OC-voltage of the string under any solar irradiance [37]. To begin the SSJ-GMPPT, initializing the operating voltage is necessary which is shown as O_s in Fig. 3. Then, the SSJ-GMPPT operates the following three processes.

Searching Process: With the IncCond method, the first local PPP is found (M_1 in Fig. 3). The power and voltage of the PPP is recorded as P_m and V_m. Then the operating voltage is disturbed in forward direction. When the sign of *dp*/*dv* changes from negative to positive, the corresponding section-dividing point (SDP) after PPP is found (A_1 in Fig. 3). The current of SDP, is the SC-current of (j+1)th PV module (I_{sc2} in Fig. 3).

Skipping Process: As shown in Fig. 3, according to the equipower line , the algorithm in this process skips from SDP and sets the quotient of $P_m/I_{sc(j+1)}$ as the new operating voltage (B_1 in Fig. 3) . The interval between A_1 and B_1 is unnecessary to scan. That is because, $P_m = V_{B1}I_{sc2}$, the voltage and current between A_1 and B_1 is smaller than the voltage V_{B1} and current I_{sc2}, respectively. As a result, the power of the points between A_1 and B_1 is less than P_m. And then, the comparison between the new V_{ref} and V_{end} is made. If V_{ref} is higher than V_{end}, that means the GMPP has been found. Otherwise, the algorithm turns to next process. The skipping process utilizes the equipower line to skip the interval from A_1 to B_1, saves the tracking time.

Judging Process. The judging process utilizes the equation (5). It is important to note that the factor of 0.85 instead of 0.9 in (5) is used, because 0.9 is an approximate factor. To ensure the tracking accuracy of SSJ-GMPPT method, the factor of 0.85 is carefully selected. But the factor may vary in the practical PV systems accordingly. The necessary conditions to judge including $I_{B1} > 0.85I_{sc2}$ and *dp/dv* > 0. The result of the judgment would induct the algorithm to next operating process as follows:

(i) The first condition is to know whether $I_{B1} > 0.85I_{sc2}$. According to (5), for PV modules, I_m is approximately equal to $0.85{\cdot}I_{sc}$, so if $I_{B1} < 0.85I_{sc2}$, $I_{B1} < I_{m2}$, point B_1 is on the right of M_2, which means $P_{m2} < P_m$. The algorithm, then, returns to skipping process again to search the next SDP. Otherwise, $I_{B1} > 0.85I_{sc2}$, which means P_{m2} is likely larger than P_m (as shown in Fig. 3(b)). Then, the algorithm turns to the searching process to track M_2.

(ii) The second condition is to know whether *dp/dv* > 0. When $I_{B1} < 0.85I_{sc2}$, it is unnecessary to judge the sign of *dp/dv,* because it is obvious that $P_{m2} < P_m$, the algorithm turns to the skipping process. When $I_{B1} > 0.85I_{sc2}$ and *dp/dv* < 0, it is true that point B_1 is on the right of M_2, as mentioned above, and $P_{m2} < P_m$; Otherwise, B_1 is on the left of M_2 and $P_{m2} > P_m$, the algorithm will turn to the searching process for M_2.

The result of the judgment decides the different direction of algorithm. For shading pattern 1, as shown in Fig. 3(a), because $I_{B1} < 0.85I_{sc2}$ and *dp/dv* > 0, the process from A_1 to B_1 has skipped one or more PPPs (actually skip M_2). The result of the judgment would shift the program to the skipping process again. According to the constant-current property of PV module, at this time current I_{B1} can be regarded as SDP current I_{sc3} because *dp/dv* > 0 at point B_1. So the algorithm turns to the skipping process and sets the operating voltage equal to the quotient of P_m/I_{sc3}. Then, in judging process, the voltage of P_m/I_{sc3} is higher than V_{end}, so the algorithm is ended and V_{m1} is the actual voltage of GMPP. The PV string operates on M_1 and successfully tracks the GMPP. The whole scanning process in shading pattern 1 shown in Fig. 3(a) needs two tracking rounds of SSJ-GMPPT method.

For shading pattern 2, as shown in Fig. 3(b), because $I_{B1} > 0.85I_{sc2}$ and *dp/dv* > 0, point B_1 lies on the left of M_2, which means the power of the second PPP (P_{m2}) is higher than the recorded P_m. The algorithm would turn to the searching process again. The newly obtained PPP and SDP are M_2 and A_2. Because P_m/I_{sc3} is higher than V_{end}, the second judging result is that M_2 is the GMPP and voltage vicinity of M_3 is unnecessary to scan. The algorithm would operate on M_2 which is actually the GMPP. The whole scanning process in shading pattern 2 spends two tracking rounds of SSJ-GMPPT method.

For shading pattern 3, as shown in Fig. 3(c), because $I_{B1} < 0.85I_{sc2}$ and *dp/dv* > 0, the process from A_1 to B_1 has skipped M_2. The program would turn to the skipping process again. The current of B_1 is regarded as the current of second SDP. In the skipping process for the second time, the operating voltage changes from B_1 to B_2 which is achieved by the quotient of P_m/I_{sc3}. In the judging process for the second time, because $I_{B2} > 0.85I_{sc3}$ and *dp/dv* > 0, point B_2 lies on the left of M_3, which means the power of the third PPP (P_{m3}) is higher than the recorded P_m. The program would turn to the searching process for M_3. Once M_3 is obtained and P_{m3} is recorded, the disturbance will be done to search the next SDP. However, as M_3 is the last one PPP, the operating voltage will reach V_{end} during the disturbance. As a result, the algorithm will be ended. The obtained GMPP is M_3. The whole scanning process in shading pattern 3 spends three tracking rounds of SSJ-GMPPT method.

This article has been accepted for publication in a future issue of this journal, but has not been fully edited. Content may change prior to final publication. Citation information: DOI 10.1109/TIE.2015.2465897, IEEE Transactions on Industrial Electronics

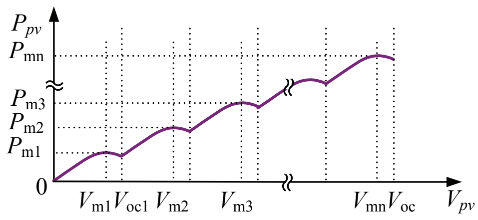

Fig. 5. Special case of output property of PV string with n modules in series.

The restart conditions of SSJ-GMPPT method includes two: one condition is that restart of method periodically occurs every 15 minutes to eliminate the gradually accumulated error caused by ambient environment or truncation error in digital processing [6], [30], and the other restart condition is set by comparing the real power and obtained global maximum power as shown:

$$\Delta p = \frac{|P_{in} - P_{m}|}{P_{m}} \qquad (7)$$

if Δp>0.1, the ambient irradiance mutation or shading conditions is considered to occur, then the method restart to the initial operation point.

In the three processes of the SSJ-GMPPT the searching process consumes the time to ensure the system attains steady state before the next MPPT perturbation begins. The skipping and judging process save time by skipping the voltage intervals which are necessary to scan, such as M_2 and M_3 vicinity in pattern 1, M_3 vicinity in pattern 2, and M_2 vicinity in pattern 3. Thus, the searching voltage range is reduced and the tracking time of GMPP can be saved in some extent. As for the string with more modules, SSJ-GMPPT method can also find and track the GMPP by repeating the three processes. Furthermore, the lower the voltage of GMPP is, the less rounds the method repeats, and less time the process of tracking spends.

IV. Rapid Global MPPT Method under PSC

When the voltage of GMPP is lower, the SSJ-GMPPT proposed in Section III needs fewer rounds to track GMPP, But if the voltage of GMPP is very high, and especially for long PV string, the method may be inefficient. For example, if the powers of the PPPs increases one by one, as shown in Fig. 5, the scanning time may be longer because the algorithm must sequentially scans every PPP.

In order to overcome the drawback of the SSJ-GMPPT for long PV string under PSC, this section proposes a rapid global MPPT method (R-GMPPT) based on the approximate voltage relationship expressed in (6).

According to (6), for the string with n modules under PSC, there are n PPPs in the P-V curve. These voltage values V_{mj} of PPP can be approximately pre-estimated by (6).

The approximate power values of all PPPs can be pre-estimated by $V_{mj}I_{mj}$, as shown in (8), in which I_{mj} can be determined by I_{scj} during the algorithm initialization based on (5). In the algorithm initialization, the operating voltage is set as 60%$V_{oc\text{-}mod}$, which can make all shaded PV modules operating in short-circuit. So I_{scj} can be measured by subtracting the current of bypass diode from string current (As seen in Fig. 2(a), $I_{sc1}= i_{str}- i_{dp1}$, $I_{sc2}= i_{str} - i_{dp2}$).

$$P_{mj} = V_{mj} I_{mj} \approx \left[(j - 0.24)V_{oc}/n\right]\left[0.9 I_{scj}\right] \qquad (8)$$

With the obtained P_{mj}, the approximate global maximum

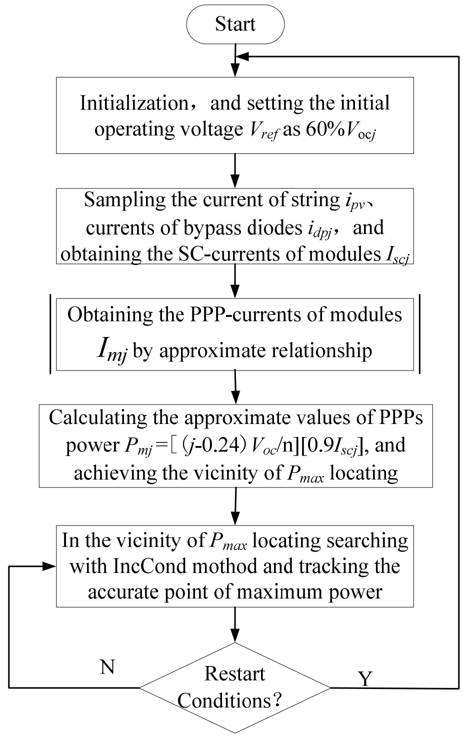

Fig. 6. Complete algorithm flowchart of R-GMPPT.

power point (AGMPP) can be distinguished. Then the IncCond method is used to accurately track the GMPP in the local vicinity of the AGMPP. As a result, the accurate GMPP would be obtained.

The flow diagram of R-GMPPT is shown in Fig. 6. The initialization, ending condition and restart condition are same as SSJ-GMPPT method. In this method, the voltage interval of scanning is greatly reduced and only the vicinity of the AGMPP is necessary to search which is greatly less than that of the conventional searching method. Therefore, by applying only one local-scanning to replace the global-scanning, the searching time is substantially shortened. It should be noted that the R-GMPPT method needs n current sensors to measure the bypass diode current, leading to a increased cost. The OC-voltage of PV string should be updated for every PV system maintenance such as every half a year to eliminate the OC-voltage error by aging.

V. Experimental Verification

To validate the performance of the proposed SSJ-GMPPT and R-GMPPT methods, a prototype with 1 kW output power is designed and fabricated in the lab. The boost converter is chosen as the power stage and the algorithms of SSJ-GMPPT and R-GMPPT are realized by a micro-controller, as shown in Fig. 7. The converter parameters are listed in Table I. A PV simulator of 62150H- 600S is used for imitating the output of PV string under PSC which includes 3 modules in series. The parameters of string under standard conditions list in Table II. For comparison, two other methods based on IncCond method, amed conventional global IncCond (C-GMPPT) and modified global IncCond (M-GMPPT), is used to track the GMPP for the PV string under the same partially shaded conditions. The C-GMPPT method regularly scans the voltage range from initial operation point to the ending point with conventional IncCond method [6]. The M-GMPPT method is mainly proposed in [27] with the outstanding performance of tracking accuracy and tracking speed. The M-GMPPT method utilizes

This article has been accepted for publication in a future issue of this journal, but has not been fully edited. Content may change prior to final publication. Citation information: DOI 10.1109/TIE.2015.2465897, IEEE Transactions on Industrial Electronics

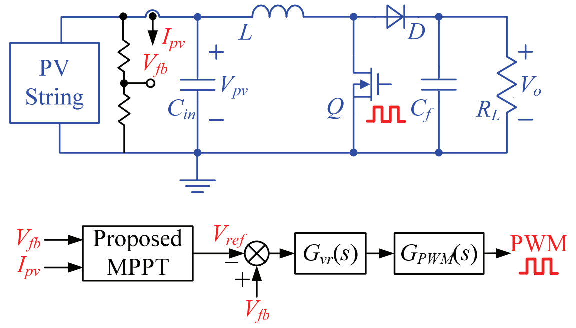

Fig. 7. Experimental setup and system block diagram.

the characteristic of PV string, peaks in the P-V curve occurring approximately at the multiples of 80% of OC-voltage of PV module, to scan the vicinity of each PPP by increasing $0.8V_{\text{oc-mod}}$ every time. To fair comparison, the converter switching frequency (100kHz) and voltage increment (0.2V) are same each other. Furthermore, to ensure the system attains steady state before the next MPPT perturbation is initiated, the sampling interval is chosen as 0.01 s (1000 switching cycles).

A. Experimental Results of Irradiance Mutation

At the beginning, the PV string including three modules with uniform irradiance is controlled to track the only MPP and operate on the V_m. At this time, a shadow appears and one of three modules is seriously shaded. The output property of string is clearly changed as shown in Fig. 8. The methods of SSJ-GMPPT and R-GMPPT can detect the change and restart to search the global MPP and operate on new voltage. After a short while, the shadow disappears and the irradiance becomes uniform again. The two methods also restart to operate on the former MPP.

Fig. 9 shows the process previously mentioned. At 1.2 second, the shadow appears, and the two methods restart to search the global MPP in 1 second and 0.1 second, respectively. After a short while, the shadow disappears, and the system returns to the condition of uniform irradiance and the two methods restart to search the former MPP.

B. Experimental Results of MPPT Methods under Different Shading Patterns

TABLE I
PARAMETERS OF THE PROTOTYPE

Parameter	Value	Parameter	Value
Input voltage V_{in}/V	20-110	Inductor L/μH	200
Output power P_o/W	1000	Input capacitor C_{in}/μF	200
Switching frequency f_s/kHz	100	Filter capacitor C_f/μF	440

TABLE II
PARAMETERS OF PV STRING UNDER STANDARD CONDITIONS

Parameter	Value	Parameter	Value
OC-voltage of module V_{ocj}/V	41.5	OC-voltage of string V_{oc}/V	124.5
SC-current of module I_{scj}/A	11.05	SC-current of string I_{sc}/A	11.05
PPP-Voltage of module V_{mj}/V	33.7	PPP-voltage of string V_m/V	101.1
PPP-Current of module I_{mj}/A	10.32	PPP-current of string I_m/A	10.32
PPP-power of module P_{mj}/W	347.4	PPP-power of string P_m/W	1042.2

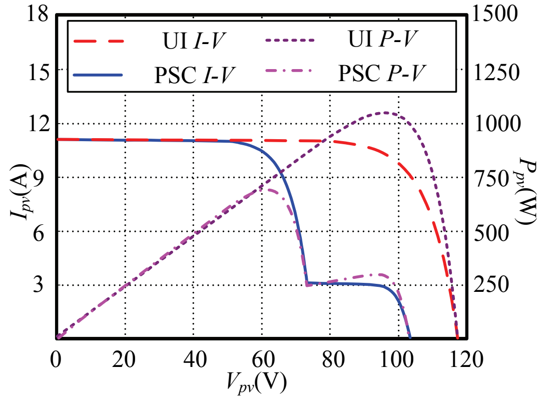

Fig. 8. Output characteristics of PV string under uniform illumination and partial shading

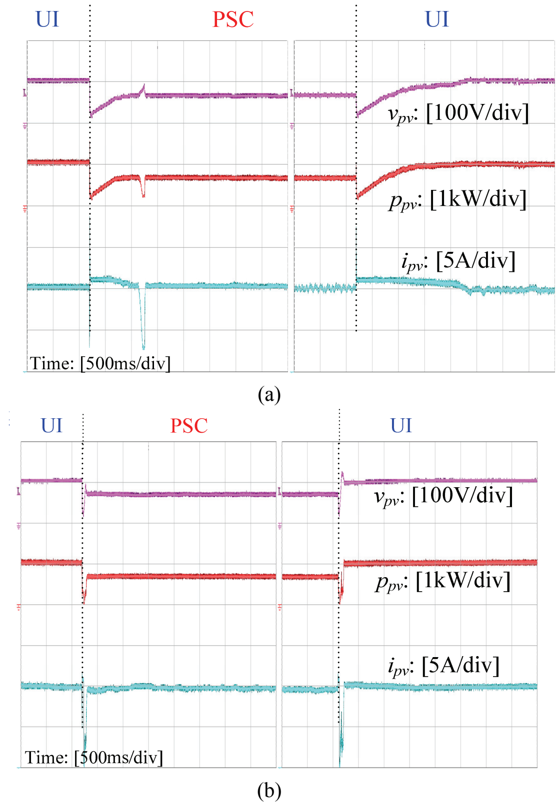

Fig. 9. Tracking results under changed shading case. (a) SSJ-GMPPT. (b) R-GMPPT.

Three shading patterns under PSC, the same as that in Section III, are simulated here, in which the GMPP is the first, second and third PPP, respectively. Fig. 10(a), (b) and (c) shows the performance of four MPPT methods under shading pattern 1, 2 and 3, respectively.

Fig. 10(a) shows the performance of four methods to track GMPP under shading pattern 1. C-GMPPT method regularly scans the P-V curve from the 60% of $V_{\text{oc-mod}}$ (24.9 V) to the 90% OC-voltage of the string (112 V) with IncCond method. The algorithm finally operates on the first PPP (GMPP) whose voltage and power are 33.5 V and 339 W, respectively. The perturbation includes 124 steps and whole operation time of tracking GMPP spends 1.24 seconds. It should be noted that in order to fast scan the full voltage range the voltage increment in C-GMPPT method is adjusted to 0.8V.

Under shading pattern 1, M-GMPPT method scans the P-V curve from the initial voltage with IncCond method and finds the first PPP. From the voltage of the first PPP the algorithm directly skips to the vicinity of the second PPP with voltage increment of $0.8V_{\text{oc-mod}}$ (33.2 V). Then with IncCond method

This article has been accepted for publication in a future issue of this journal, but has not been fully edited. Content may change prior to final publication. Citation information: DOI 10.1109/TIE.2015.2465897, IEEE Transactions on Industrial Electronics

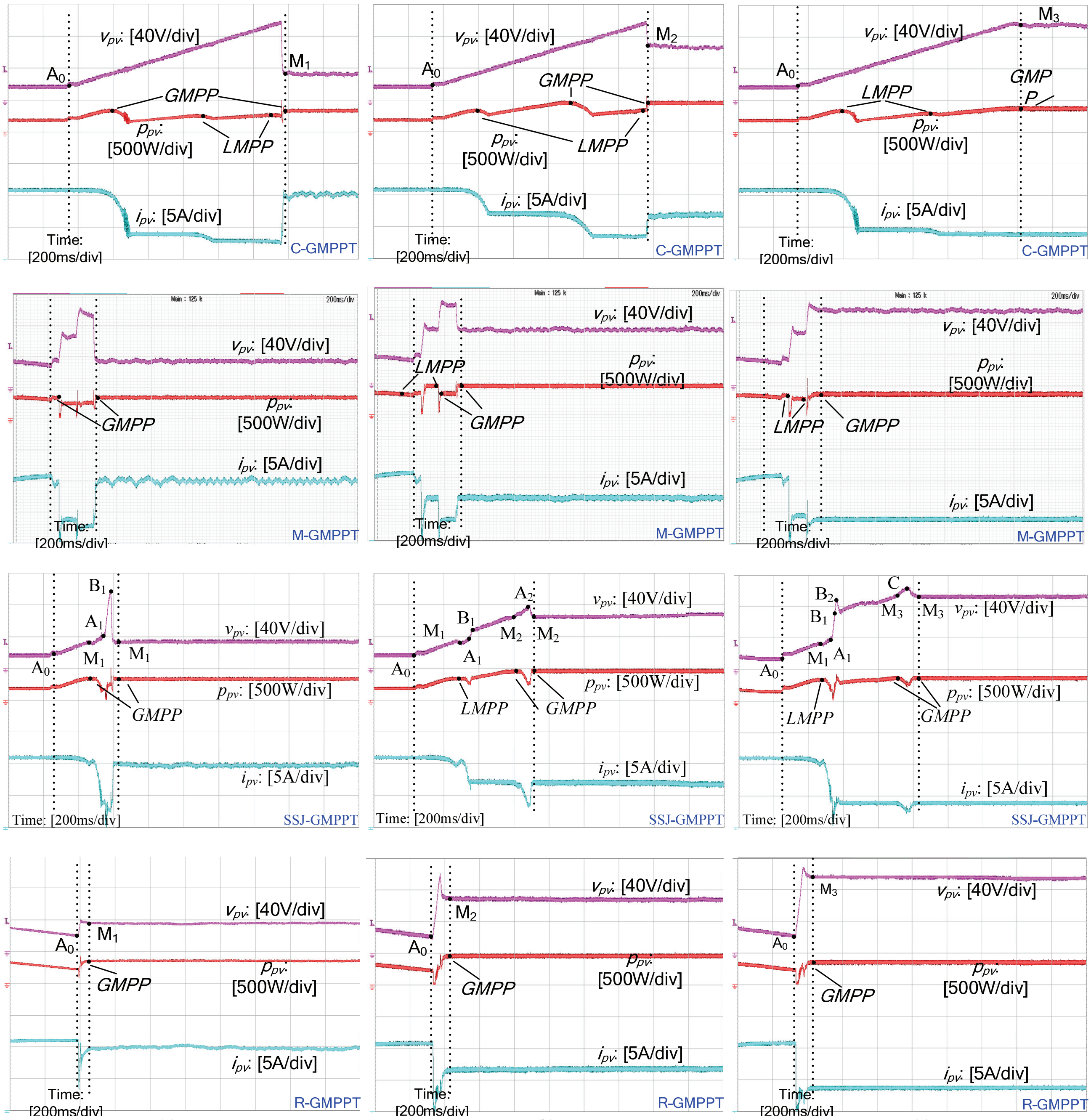

Fig. 10. Tracking performance of the four methods under the three different shading patterns. (a) pattern 1, (b) pattern 2, (c) pattern 3.

the second PPP is found with power of 258 W. From the second PPP the algorithm directly skips to the vicinity of the third PPP with voltage increment of $0.8V_{\text{oc-mod}}$ (33.2 V). Then with IncCond method the third PPP is found with power of 266 W. The algorithm finally turns to the first PPP which is GMPP with voltage 33.5 V and power 339 W. The perturbation includes 27 steps and whole operation time of tracking GMPP spends 0.27 seconds.

Under shading pattern 1, SSJ-GMPPT methods scans the P-V curve from the the 60% of $V_{\text{oc-mod}}$ (24.9V) with IncCond method and finds the first PPP (M_1). The voltage (33.5 V) and power (339 W) of the first PPP is recorded as P_{m} and V_{m}. Then the operating voltage is disturbed in forward direction until the first SDP (A_1) is found. The current of SDP is 4 A which means I_{sc2} is 4 A. The algorithm sets the quotient of $P_{\text{m}}/I_{\text{sc2}}$ (84.75 V) as the new operating voltage (B_1). The voltage interval between A_1 and B_1 is skipped. Because I_{B1} (1.4 A) < $0.85I_{\text{sc2}}$ and dp/dv > 0, the method begins to skip again. The current of I_{B1} is approximately equal to I_{sc3}. Set the quotient of $P_{\text{m}}/I_{\text{sc3}}$ (242 V) as the new operating voltage. The quotient is higher than V_{end} (112V) so the method finally turns to the first PPP which is GMPP with voltage and power of 33.5 V and 339 W. The perturbation includes 38 steps and whole operation time of tracking GMPP spends 0.38 seconds.

Under shading pattern 1, R-GMPPT sets the 60% of $V_{\text{oc-mod}}$ (24.9V) as initial operation voltage in order to ensure almost shaded modules bypassed. Then, by measuring the current of PV string and three bypass diodes, the SC-current of each module is obtained. Then each P_{mj} is calculated and P_{m1} (339 W), P_{m2} (254 W) and P_{m3} (275 W) are obtained according to (8). So the AGMPP is obtained whose voltage is $0.76V_{ocj}$=31.54 V. Then with IncCond method the GMPP with voltage and power of 33.5 V and 339 W is found. The perturbation includes only 6 steps and whole operation time of tracking GMPP spends 0.06 seconds.

This article has been accepted for publication in a future issue of this journal, but has not been fully edited. Content may change prior to final publication. Citation information: DOI 10.1109/TIE.2015.2465897, IEEE Transactions on Industrial Electronics

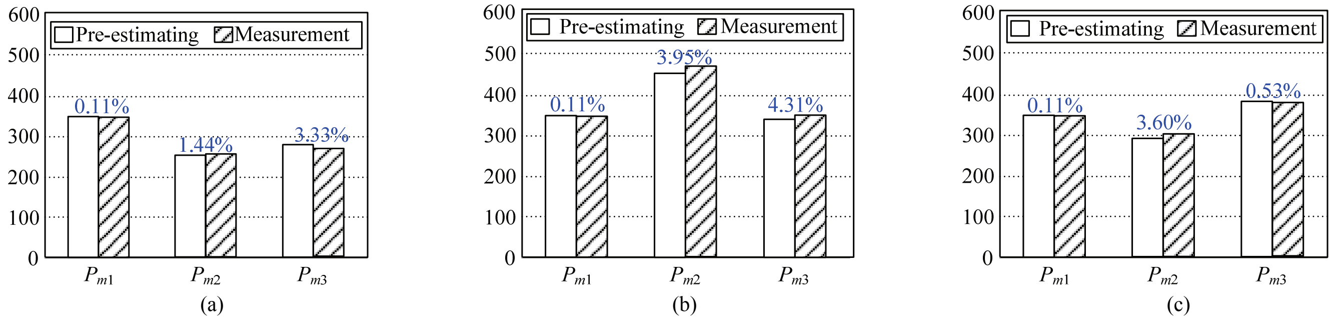

Fig. 11. Differences between pre-estimating and real values in three shadow patterns. (a) pattern 1, (b) pattern 2, (c) pattern 3.

TABLE III
PERFORMANCE COMPARISON OF FOUR MPPT METHODS UNDER DIFFERENT SHADING PATTERNS

Shading pattern	MPPT method	Perturbation Steps	Tracking speed	Tracking efficiency	Implementing complexity	Required additional sensor
1	C-GMPPT	124	slow			none
	M-GMPPT	27	fast			none
	SSJ-GMPPT	38	fast			none
	R-GMPPT	6	very fast			current sensors
2	C-GMPPT	124	slow			none
	M-GMPPT	27	fast	99.5%	simple	none
	SSJ-GMPPT	58	medium			none
	R-GMPPT	8	very fast			current sensors
3	C-GMPPT	124	slow			none
	M-GMPPT	22	fast			none
	SSJ-GMPPT	76	medium			none
	R-GMPPT	7	very fast			current sensors

For shading pattern 2 and 3, the whole tracking processes are shown in Fig. 10(b) and (c), respectively. Every method successfully tracks the global MPP in two patterns. The transient response curve shows the robustness of the proposed algorithms irrespective of the shading pattern.

A quantitative comparison of four global MPPT methods is given in Table III. In this table, the tracking efficiency is defined as the ratio between averaged output power obtained under steady state and maximum available power of the PV string under PSC. The tracking efficiency that can be directly observed in the PV simulator window reflects the tracking accuracy of MPPT methods. Due to the IncCond method utilization to find GMPP, the tracking efficiency of four methods are same which reach 99.5%. However, the tracking speed is different.

C. Tracking Speed of Four Methods under PSC

The tracking speed of GMPP depends on the voltage range need to be scanned. The C-GMPPT method scans the whole voltage range from initial point to the ending point so that its tracking speed is slow. The M-GMPPT method only scans the voltage vicinity of near every PPP, so the tracking speed is improved. The SSJ-GMPPT method skips the local PPPs whose power are less than the recorded maximum power value, so the tracking speed of SSJ-GMPPT is faster than that of C-GMPPT. But under some irradiance, the SSJ-GMPPT may not skip enough PPPs such as the given example shown in Fig. 5, resulting in longer tracking time. The R-GMPPT only scans the vicinity of one PPP which is distinguished in *n* PPPs based on the approximately estimated power values. It is obvious that the R-GMPPT method scans the least voltage range and the tracking speed is the fastest. Moreover, the scanning voltage range and time of R-GMPPT is not changed with more modules in a PV string while other three methods inevitably increase the scanning voltage range and tracking time. Thus, in consideration of outstanding tracking speed, the R-GMPPT method is suitable for the long PV string with plenty of modules.

D. Tracking Accuracy of Four Methods under PSC

In term of tracking accuracy the C-GMPPT method scans the whole voltage range and real GMPP is guaranteed. The M-GMPPT scans vicinity of every PPP and the GMPP is one of PPPs, which means the GMPP can be tracked accurately. The SSJ-GMPPT scans partial PPPs whose power are more than the recorded power in whole tracking process, which ensures the GMPP is not missed. All of three methods above exhibit high tracking accuracy. In the process of R-GMPPT, the approximate value of V_{mj} and I_{mj} would bring a little difference between the pre-estimated P_{mj} value and measured P_{mj} value. The difference may result in the algorithm misjudging and influence the accuracy of R-GMPPT. The differences in three shading patterns are shown in Fig.11. For the R-GMPPT, a conventional IncCond method is utilized to eliminate these differences. So, the tracking accuracy is guaranteed to be promoted. With regard of tracking accuracy and speed, the M-GMPPT and

SSJ-GMPPT are preferable to be utilized in the conditions of PV popular string.

VI. CONCLUSION

The P-V curve of PV string under partially shaded conditions exhibits multiple peaks. Conventional MPPT methods are unable to achieve either sufficient accuracy or fast tracking speed. In this paper, two global MPPT methods, SSJ-GMPPT and R-GMPPT methods, are proposed in term of reducing the searching voltage range based on comprehensive study of I-V and P-V characteristics of PV string. The SSJ-GMPPT method is capable of tracking the global maximum power point with high accuracy and approving speed without additional circuit and sensor. The R-GMPPT method exhibits very fast tracking speed with 90% time saved compared to the conventional global MPPT method, so it can be used in the conditions of long PV string. The experimental results and comparison with other methods have verified the performance of proposed MPPT methods. The SSJ-GMPPT method guarantees tracking accuracy with an approving tracking time, while R-GMPPT method performs at a higher speed with acceptable accuracy.

REFERENCES

[1] D. S. Sun, B. M. Ge, X. Y. Yan, D. Q. Bi, H. Zhang, Y. S. Liu, A. B. H, B. B. L, and F. Z. Peng, "Modeling, impedance design, and efficiency analysis of quasi-Z source module in cascaded multilevel photovoltaic power system," *IEEE Trans. Ind. Electron.*, vol. 61, no. 11, pp. 6108-6117, Nov. 2014.

[2] M. Boztepe, F. Guinjoan, G. Velasco-Quesada, S. Silvestre, A. Chouder, and E. Karatepe, "Global MPPT scheme for Photovoltaic string inverters based on restricted voltage window search algorithm," *IEEE Trans. Ind. Electron*., vol. 61, no. 7, pp. 3302-3312, Jul. 2014.

[3] A. Maki and S. Valkealahti, "Power losses in long string and parallel-connected short strings of series-connected silicon-based photovoltaic modules due to partial shading conditions," *IEEE Trans. Energy Convers.*, vol. 27, no. 1, pp. 173-183, Mar. 2012.

[4] E. Mamarelis, G. Petrone, and G. Spagnuolo, "Design of a sliding-mode-controlled SEPIC for PV MPPT applications," *IEEE Trans. Ind. Electron*., vol. 61, no. 7, pp. 3387-3398, Jul. 2014.

[5] M. A. G. de Brito, L. Galotto, L. P. Sampaio, G. A. E Melo, and C. A. Canesin, "Evaluation of the main MPPT techniques for photovoltaic applications," *IEEE Trans. Ind. Electron*., vol. 60, no. 3, pp. 1156-1167, Mar. 2013.

[6] E. Koutroulis and F. Blaabjerg, "A new techniques for tracking the global maximum power point of PV arrays operating under partial-shading conditions," *IEEE J. Photovolt.*, vol. 2, no. 2, Apr. 2012.

[7] T. Shimizu, M. Hirakata, T. Kamezawa, and H. Watanabe, "Generation control circuit for photovoltaic modules," *IEEE Trans. Power Electro.*, vol. 16, no. 3, pp. 293-300, May. 2001.

[8] E. Karatepe, T. Hiyama, M. Boztepe, and M. Colak, "Voltage based power compensation system for photovoltaic generation system under partially shaded insolation conditions," *Energy Convers. Manag.*, vol. 49, no. 8, pp. 2307-2316, Aug. 2008.

[9] P. Sharma and V. Agarwal, "Maximum power extraction from a partially shaded PV array using shunt-series compensation," *IEEE J. Photovolt.,* vol. 4, no. 4, pp. 1128-1137, Jul. 2014.

[10] P. Sharma and V. Argarwal, "Exact maximum power point tracking of grid-connected partially shaded PV source using current compensation concept, " *IEEE Trans. Power Electro.*, vol. 29, no. 9, pp. 4684-4692, Sep. 2014.

[11] M.Z.S. El-Dein, M. Kazerani, and M.M.A. Salama, "Optimal photovoltaic array reconfiguration to reduce partial shading losses," *IEEE Trans. Sustain. Energy*, vol. 4, no. 1, pp. 145−153, Jan. 2013.

[12] Y. Hu, H. Chen, R. D. Xu, and R. Li, "Photovoltaic (PV) array fault diagnosis strategy based on optimal sensor placement," *Proceedings of CSEE*, vol. 31, no. 33, pp. 19−30, Nov. 2011.

[13] G. Velasco-Quesada, F. Guinjoan-Gispert, R. Pique-Lopez, M. Roman-Lumbreras, and A. Conesa-Roca, "Electrical PV array reconfiguration strategy for energy extraction improvement in grid-connected PV systems," *IEEE Trans. Ind. Electron*., vol. 56, no. 11, pp. 4319-4331, Nov. 2009.

[14] S. R. Shubhajit and H. Saha, "Maximum power point tracking of partially shaded solar photovoltaic arrays," *Solar Energy Mater. Solar Cells*, vol. 94, no. 9, pp. 1441-1447, Sep. 2010.

[15] Y. Liu, S. Huang, and W. Liang, "A particle swarm optimization-based maximum power point tracking algorithm for PV systems operating under partially shaded conditions," *IEEE Trans. Energy Convers.*, vol. 27, no. 4, pp. 1027-1035, Dce. 2012.

[16] K. Ishaque, Z. Salam, M. Amjad, and S. Mekhilef, "An improved particle swarm optimization (PSO)–based MPPT for PV with reduced steady-state oscillation," *IEEE Trans. Power Electron.*, vol. 27, no. 8, pp. 3627-3638, Aug. 2012.

[17] K. Sundareswaran, S. Peddapati, and S. Palani, "MPPT of PV systems under partial shaded conditions through a colony of flashing fireflies," *IEEE Trans. Energy Convers.*, vol. 29, no. 2, pp. 463-472, Jun. 2014.

[18] K. Sundareswarm, P. Sankar, P. S. R. Nayak, S. P. Simon, and S. Palani, "Enhanced energy output from a PV system under partial shaded conditions through artificial bee colony," *IEEE Trans. Sustain. Energy*, vol. 6, no. 1, pp. 198−209, Jan. 2015.

[19] B. N. Alajmi, K. H. Ahmed, S. J. Finney, and B. W. Williams, "A maximum power point tracking technique for partially shaded photovoltaic systems in microgrids," *IEEE Trans. Ind. Electron.*, vol. 60, no.4, pp. 1596-1606, Apr. 2013.

[20] L. Zhou, Y. Chen, K. Guo, and F. Jia, "New approach for MPPT control of photovoltaic system with mutative-scale dual-carrier chaotic search," *IEEE Trans. Power Electron.*, vol. 26, no. 4, pp. 1038-1048, Apr. 2011.

[21] K. Kobayashi, I. Takano, and Y. Sawada, "A study of a two-stage maximum power point tracking control of a photovoltaic system under partially shaded insolation conditions," *Solar Energy Mater. Solar Cells*, vol.90, no. 18-19, pp. 2975-2988, Nov. 2006.

[22] Y. H. Ji, D. Y. Jung, J. G. Kim, J. H. Kim, T. W. Lee, and C. Y. Won, "A real maximum power point tracking method for mismatching compensation in PV array under partially shaded conditions," *IEEE Trans. Power Electron.*, vol. 26, no. 4, pp. 1001-1009, Apr. 2011.

[23] T. L. Nguyen and K. S. Low, "A global maximum power point tracking scheme employing DIRECT search algorithm for photovoltaic systems," *IEEE Trans. Ind. Electron.*, vol. 57, no. 10, pp. 3456-3467, Oct. 2010.

[24] N. A. Ahmed and M. Miyatake, "A novel maximum power point tracking for photovoltaic applications under partially shaded insolation conditions," *Electr. Power Syst. Res.*, vol. 78, no. 5, pp. 777-784, May. 2008.

[25] K. Ishaque and Z. Salam, "A deterministic particle swarm optimization maximum power point tracker for photovoltaic system under partial shading condition," *IEEE Trans. Ind. Electron.*, vol. 60, n. 8, pp. 3195-3206, Aug. 2013.

[26] H. Patel and V. Agarwal, "Maximum power point tracking scheme for PV systems operating under partially shaded conditions," *IEEE Trans. Ind. Electron.*, vol. 55, no. 4, pp. 1689-1698, Apr. 2008.

[27] K. S. Tey and S. Mekhilef, "Modified incremental conductance algorithm for photovoltaic system under partial shading conditions and load variation," *IEEE Trans. Ind. Electron.*, vol. 61, n. 10, pp. 5384-5392, Oct. 2014.

[28] K. S. Tey and S. Mekhilef, "A fast-converging MPPT technique for photovoltaic system under fast-varying solar irradiation and load resistance," *IEEE Trans. Ind. Informa.*, vol. 11, n. 1, pp. 176-186, Feb. 2014.

[29] K. S. Tey and S. Mekhilef, "Modified incremental conductance MPPT algorithm to mitigate inaccurate responses under fast-changing solar irradiation level Solar Energy," Elsevier, vol. 101, pp. 333-342, 2014.

[30] K. S. Tey, S. Mekhilef, and A. Safari, "Simple and low cost incremental conductance maximum power point tracking using buck-boost converter," *Journal of Renewable Sustainable Energy* 5, 023106 (2013).

[31] M. Seyedmahmoudian, S. Mekhilef, R. Rahmani, R. Yusof, and E. T. Renani, "Analytical modeling of partially shaded photovoltaic systems," Energies, vol. 6, n. 1, pp. 128-144, Jun. 2013.

[32] A. Bidram, A. Davoudi, and R.S. Balog, "Control and circuit techniques to mitigate partial shading effects in photovoltaic arrays," *IEEE J. Photovolt.,* vol. 2, no. 4, pp. 532−546, Oct. 2012.

[33] S. Lineykin, M. Averbukh, and A. Kuperman, "Issues in modeling amorphous silicon photovoltaic modules by single-diode equivalent circuit," *IEEE Trans. Ind. Electron*., vol. 61, no. 12, pp. 6785-6793, Dec. 2014.

[34] M. A. Masoum, H. Dehbonei, and E. F. Fuchs, "Theoretical and experimental analyses of photovoltaic systems with voltage- and current-based maximum power-point tracking," *IEEE Trans. Energy Convers.*, vol. 17, no. 4, pp. 514-522, Dec. 2002.

[35] J. Ding, X. Cheng, Z. Zhai, J. Zha, and M. Mao, "Theoretical analysis

This article has been accepted for publication in a future issue of this journal, but has not been fully edited. Content may change prior to final publication. Citation information: DOI 10.1109/TIE.2015.2465897, IEEE Transactions on Industrial Electronics

and calculation for filling factor of solar cell varying along with illumination intensity," *Engineering Science*, vol. 9, no. 6, pp. 82-87, Jun. 2007.

[36] J. C. Wang, Y. L. Su, K. C. Kuo, J. C. Shieh, and J. A. Jiang, "A novel multipoint direct-estimation method for the maximum power point tracking of photovoltaic modules under partially shaded irradiation conditions," in *Proc. IEEE International Energy Conference & Exhibition (ENERGYCON)*, 2012, pp. 13–19.

[37] S. Lyden, M. E. Haque, A. Gargoom, and M. Negnevitsky, "Review of maximum power point tracking approaches suitable for PV systems under partial shading conditions," in *Proc. Aus. Univer. Power Engineer. Conf. (AUPEC)*, 2013, pp. 1–6.

Yunping Wang was born in Henan Province, China, in 1979. He received the B.S. in measuring and controlling device in 2002, and M.S. degrees in power electronics in 2007, from Nanjing University of Aeronautics and Astronautics (NUAA), Nanjing, China, where he is currently working toward the Ph.D. degree in electrical engineering.

His current research interests include the Photovoltaic generation system.

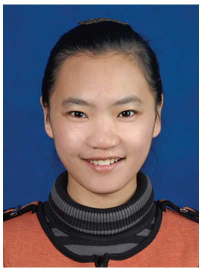

Ying Li (S'15) was born in Jiangsu Province, China, in 1992. She received the B. S. degrees in electrical engineering and automation from Nanjing University of Aeronautics and Astroniatics (NUAA), Nanjing, China, in 2014, where she is currently working toward the Ph.D degree in electrical engineering.

Her current research interests include high frequency power conversion and resonant converters.

Xinbo Ruan (SM'02) received the B.S. and Ph.D. degrees in electrical engineering from Nanjing University of Aeronautics and Astronautics (NUAA), Nanjing, China, in 1991 and 1996, respectively.

In 1996, he joined the College of Automation Engineering, NUAA, where he became a Professor in 2002. From 2008 to 2011, he was also with the College of Electrical and Electronic Engineering, Huazhong University of Science and Technology, Wuhan, China. He is the author or co-author of seven books and more than 180 technical papers published in journals and conferences. His main research interests include soft-switching power electronics converters, power electronics system integration and renewable energy generation system.

From 2005 to 2013, he served as Vice President of the China Power Supply Society. He has been an Associate Editor for the IEEE Transactions on Industrial Electronics and the IEEE Journal of Emerging and Selected Topics on Power Electronics since 2011 and 2013, respectively.